Classifying and quantifying basins of attraction

J. C. Sprott and Anda Xiong
Physics Department, University of Wisconsin-Madison, 1150 University Avenue, Madison, Wisconsin 53706, USA

A scheme is proposed to classify the basins for attractors of dynamical systems in arbitrary dimensions. There are four basic classes depending on their size and extent, and each class can be further quantified to facilitate comparisons. The calculation uses a Monte Carlo method and is applied to numerous common dissipative chaotic maps and flows in various dimensions. © 2015 AIP Publishing LLC. [http://dx.doi.org/10.1063/1.4927643]

In the modern chaos era, hundreds of examples of dissipative dynamical systems with strange attractors have been proposed and described. These descriptions often include plots of the attractor, Lyapunov exponents, attractor dimension, equilibria and their eigenvalues, bifurcations, and routes to chaos. Less often is attention given to the basin of attraction despite the fact that knowledge of the basin is essential for these calculations and for determining possible multistability and the usefulness of the systems in practical applications. A knowledge of the basin is especially important for the growing list of attractors that are "hidden" in the sense that the basin does not contain the small neighborhood of any unstable equilibrium points.[1,2] Thus, it is important to have a means of classifying and quantifying the size and extent of attractor basins.

I. INTRODUCTION

All attractors, whether they be stable equilibria, limit cycles, attracting tori, or strange attractors, are surrounded by a basin of attraction representing the set of initial conditions in the state space whose orbits approach and map out the attractor as time approaches infinity. Basins can be small and fit tightly around the attractor or large and include the entire state space. More typically, the basin has some intermediate size and may stretch to infinity in certain directions but only fill a portion of the available state space. The boundary of the basin can be smooth or fractal[3,4] or even riddled.[5] Initial conditions outside the basin may lie on unstable periodic orbits, approach a different coexisting attractor, or escape to infinity. In engineering applications, it is often important that the basin be large enough that there is no danger that some perturbation to the system will disrupt its dynamics with possibly dire consequences. Thus, it is important to have a means for describing the basin of attraction and quantifying its shape and size for both theoretical and practical reasons.

Here, we describe such a method which consists of calculating the probability P that an initial condition at a distance r from the attractor lies within the basin of the attractor. In particular, we focus on the behavior of the function $P(r)$ in the limit $r \to \infty$ and find that most attractors are well characterized by a power law $P(r) = P_0/r^\gamma$ in that limit. The parameters P_0 and γ serve to quantify the basin.

All the attractors examined in this way have a basin that falls into one of four classes: (1) Class 1 has $P_0 = 1, \gamma = 0$ and attracts almost all initial conditions. (2) Class 2 has $P_0 < 1, \gamma = 0$ and thus attracts a fixed fraction of the state space. (3) Class 3 has $0 < \gamma < D$, where D is the dimension of the state space and γ is the codimension of the basin (the dimension of the space not in the basin), which is not necessarily an integer. (4) Class 4 has $\gamma = D$ and a bounded basin with a fixed, well-defined linear size given in normalized form by $r_0 = P_0^{1/D}$. The four classes represent a hierarchy of basin sizes from the largest to the smallest and provide a means for comparing the size of two basins of the same class.

II. NUMERICAL METHOD

Since it is usually not possible to calculate analytically the boundary of an attractor's basin, it is necessary to resort to a numerical method. For that purpose, the Monte Carlo method[6] is well suited. In principle, one only needs to populate the interior of hyperspheres of different radii centered on the attractor with uniform random initial conditions and test what fraction of those points converge to the attractor. In practice, there are a number of issues that must be considered, especially since the goal is to quantify that probability in the limit of large r, where the fraction of such randomly chosen points that are in the basin may be vanishingly small.

To avoid a proliferation of subscripts or vectors, consider a one-dimensional example in which the attractor and its basin occupy intervals of the X axis. A suitable example is the logistic map[7] at its accumulation point (sometimes called the "Feigenbaum point")

$$X_{n+1} = A_\infty X_n(1 - X_n), \tag{1}$$

where $A_\infty = 3.5699456718\ldots$ for which the attractor is a Cantor set with a fractal dimension of about 0.538 at the onset of chaos,[8] where the Lyapunov exponent is exactly zero, and its basin is the finite interval $0 < X < 1$.

The first task is to find the "center of mass" X_m of the attractor, which in this case is given by

$$X_m = \lim_{N \to \infty} \frac{1}{N} \sum_{n=1}^{N} X_n = 0.647603\ldots \qquad (2)$$

and the standard deviation S about that point is given by

$$S = \sqrt{\lim_{N \to \infty} \frac{1}{N} \sum_{n=1}^{N} (X_n - X_m)^2} = 0.216354\ldots \qquad (3)$$

The distance of an initial condition X_0 from the attractor is given in normalized form by $r = (X_0 - X_m)/S$. If the attractor is a fixed point such that S would be zero, S can be set to unity. Note that the basin class and value of γ are not affected by the choice of normalization, but the value of P_0 will be.

Since the basin of Eq. (1) is known exactly, it is straightforward to calculate $P(r)$

$$P(r) = \begin{cases} 1 & r \leq 1.628798 \\ 0.5 + 0.814399/r & 1.628798 < r < 2.993256 \\ 2.3110275/r & r \geq 2.993256. \end{cases}$$

$$(4)$$

Since $\gamma = 1$ at large r, this is an example of a $D = 1$ Class 4 basin with a finite linear size ($r_0 = 2.3110275$) about twice the size of the attractor. Equation (4) provides a useful check of the numerical method.

To use the method where no analytic calculation of the basin boundary is possible, one begins by choosing random initial conditions uniformly distributed in a D-dimensional hypersphere of radius $r = 1$ and calculating what fraction of them lies within the basin to obtain a value for $P(1)$. Then, one considers a hypersphere of radius $r = 2$ with random initial conditions uniformly distributed in the shell between $r = 1$ and $r = 2$ and calculates what fraction of those lies within the basin to get a value of $\Delta P(1)$ from which one calculates $P(2) = P(1)(1 - 1/2^D) + \Delta P(1)/2^D$. The procedure is repeated to get ever larger values of $P(r)$ for r increasing in powers of 2. This slightly involved method is required to distinguish $P(r)$ from zero at large values of r and D with a reasonable number of initial conditions, because it ensures that there are sufficiently many initial conditions within the basin.

To determine whether an initial condition is in the basin, it is necessary to calculate a running average of the Euclidean distance $\rho(t)$ of the orbit from the center of mass of the attractor. For an initial condition in the basin, $\rho(t)$ will converge to zero, and one can safely assume it is in the basin when $\rho(t)$ becomes less than say $S/10$. For many systems, there is a single attractor, and points outside the basin diverge to infinity, which is easy to detect if $\rho(t)$ exceeds some large value such as $1000r$, which it will usually do promptly. The case in which there is a coexisting attractor is more difficult requires adding a bailout condition if $\rho(t)$ is neither converging to zero nor diverging to infinity. In fact, a byproduct of the calculation is to identify instances of multistability, which are often overlooked.

Note that the center of mass of the attractor does not, in general, lie on the attractor and may not even be within its

basin, in which case $P(0)$ would be zero, and $P(r)$ would not be a monotonically decreasing function of r except at sufficiently large values of r. There are examples of strange attractors that surround stable fixed points[9] and ones that surround conservative tori.[10] In such unusual cases, it may be necessary to consider higher moments of $\rho(r)$ since two attractors can have similar values for their centers of mass.

Having obtained $P(r)$ for values of r at integer powers of 2, all that remains is to plot $\log_2(P)$ versus $\log_2(r)$ and fit a straight line to the points at large r, which can be automated using linear regression. The intercept of that line with $\log_2(r) = 0$ then gives P_0, and the negative of its slope gives γ. Using this procedure for the logistic map in Eq. (1) gives values that agree with Eq. (4) to within a small fraction of a percent.

III. 2-D MAP EXAMPLES

For ease of visualization and speed of computation while avoiding trivial examples, we illustrate the numerical method using two-dimensional dissipative maps whose solutions are chaotic and thus whose attractors are strange (fractal). The cases are chosen to include an example of each class of basin. The extension to higher dimensions and to chaotic flows is straightforward.

A. Class 1 basin

A Class 1 basin is one in which the basin includes all of the state space except perhaps a set of finite measure. We can further subdivide these cases into ones where the excluded set has measure zero (Class 1a) and those in which it has nonzero measure (Class 1b). A chaotic system constructed to have the former property, also called "globally attracting," is the "sine-sine" map

$$\begin{aligned} X_{n+1} &= \sin X_n - \sin 2Y_n \\ Y_{n+1} &= X_n \end{aligned} \qquad (5)$$

shown in Fig. 1 with Lyapunov exponents of (0.0465, −0.0669) and a Kaplan–Yorke dimension of 1.6945. This and the following figures show $\lg(P)$ versus $\lg(r)$, where $\lg = \log_2$ is the base-2 logarithm so that the slope of the curve is $-\gamma$.

For all the examples here, the Lyapunov exponents are calculated from the Jacobian matrix using the method described by Wolf et al.[11] except that the matrix elements are determined numerically, and the calculation is run until convergence is achieved to at least four significant digits. However, the exponents and corresponding Kaplan–Yorke dimensions are included only for completeness, and the method does not depend on their values or even that the system is chaotic but only assumes that it has an attractor of some kind.

Note that Classes 1a and 1b have the same $P(r) = 1$ in the limit $r \to \infty$, but $1 - P(r)$ is identically zero for a Class 1a basin, while it typically obeys a power law $1 - P(r) = P_0/r^\gamma$ for a Class 1b basin with $r_0 = P_0^{1/\gamma}$ a measure of the linear size of the finite region not in the basin. This excluded region may be Class 2, 3, or 4, but its (hyper)volume
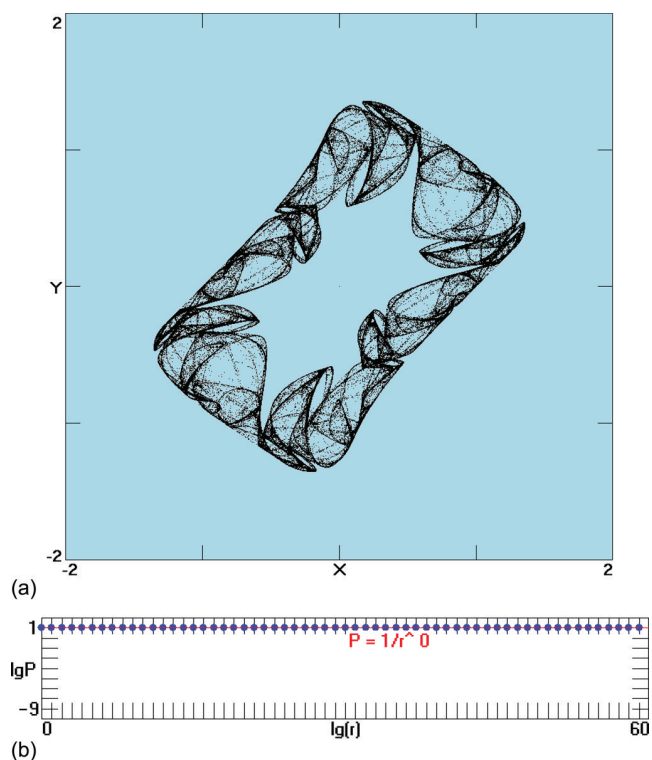
FIG. 1. The sine-sine map is globally attracting with a Class 1 basin having $P(r) = 1.0$ for all r.

FIG. 2. The Ikeda map has a Class 2 fractal basin and attracts a constant fraction of about 8% of its state space.

eventually becomes negligible compared to the (hyper)volume of the attractor basin as r increases.

For Eq. (5), almost every point in state space is on an orbit that converges to the attractor. However, there is an infinite set of points, the most obvious of which are the eventually fixed points given by $(X, Y) = (p\pi/2, q\pi/4)$, where p and q are integers, which do not approach the attractor. Furthermore, the attractor is dense in periodic points (every point on the attractor is arbitrarily close to one), all unstable. Nevertheless, the infinitely many eventually fixed and unstable periodic points are a set of measure zero in the state space, and so the basin is considered to be Class 1a. This is illustrated in Fig. 1, which shows that a point a distance r from the attractor is in the basin with probability 1.0 out to a distance of at least $r = 2^{60}$. Said differently, out of a billion randomly chosen initial conditions, not a single one failed to converge onto the attractor.

B. Class 2 basin

A Class 2 basin occupies a fixed fraction of its state space, a nontrivial example of which is the Ikeda map[12]

$$
\begin{aligned}
X_{n+1} &= \gamma + \mu(X_n \cos\phi - Y_n \sin\phi) \\
Y_{n+1} &= \mu(X_n \sin\phi + Y_n \cos\phi) \\
\phi &= \beta - a/(1 + X_n^2 + Y_n^2)
\end{aligned}
\tag{6}
$$

with $a = 6$, $\beta = 0.4$, $\gamma = 1$, and $\mu = 0.9$, as shown in Fig. 2 with Lyapunov exponents $(0.5076, -0.7183)$ and a Kaplan–Yorke dimension of 1.7066. The outer edge of the basin of attraction is a logarithmic spiral.
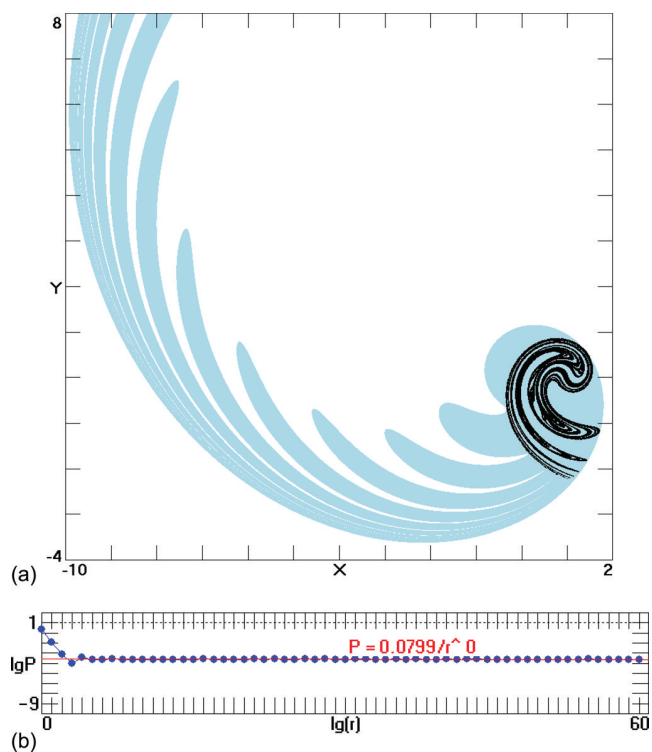
This is an example of a system in which $P(r)$ is not a monotonically decreasing function of r but rather has a small oscillation in the vicinity of $r = 8$.

C. Class 3 basin

A Class 3 basin extends to infinity in some directions but occupies an ever decreasing fraction of the state space, an example of which is the Hénon map[13]

$$
\begin{aligned}
X_{n+1} &= 1 - aX_n^2 + bY_n \\
Y_{n+1} &= X_n
\end{aligned}
\tag{7}
$$

with parameters $a = 1.4$ and $b = 0.3$, as shown in Fig. 3 with Lyapunov exponents $(0.4192, -1.6232)$ and a Kaplan–Yorke dimension of 1.2583.

Since $P(r)$ accurately follows a power law with a slope of -1.855 at large r, the basin has a fractional dimension of $D - \gamma = 2 - 1.855 = 0.145$ at the largest scale even though the basin boundary appears quite smooth.

Note that Eq. (7) has Y linearly rescaled by a factor of b from the form proposed by Hénon in order for X and Y to have the same magnitude. This transformation does not alter the dynamics or the topology of the attractor, and it preserves the value of γ, although it does give a somewhat different value of P_0 since it alters the aspect ratio of the attractor.

D. Class 4 basin

A Class 4 basin is finite in extent and thus has a well defined size in comparison with the attractor, an example of which is the Tinkerbell map[14]
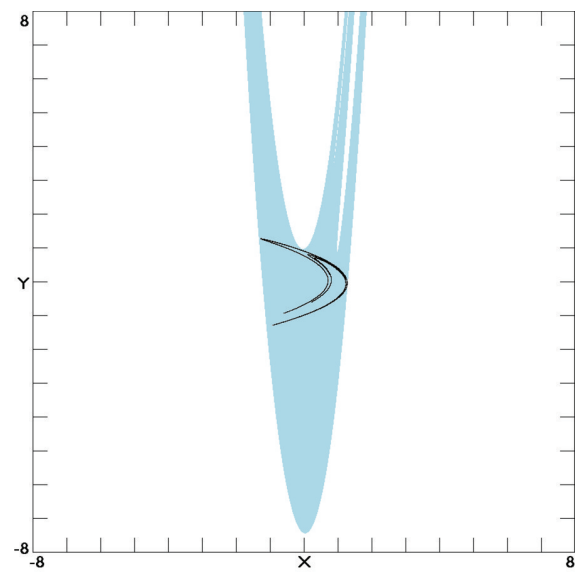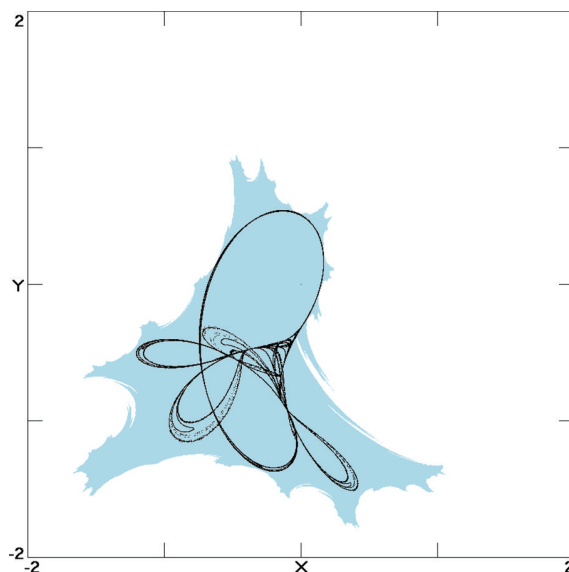
(a)
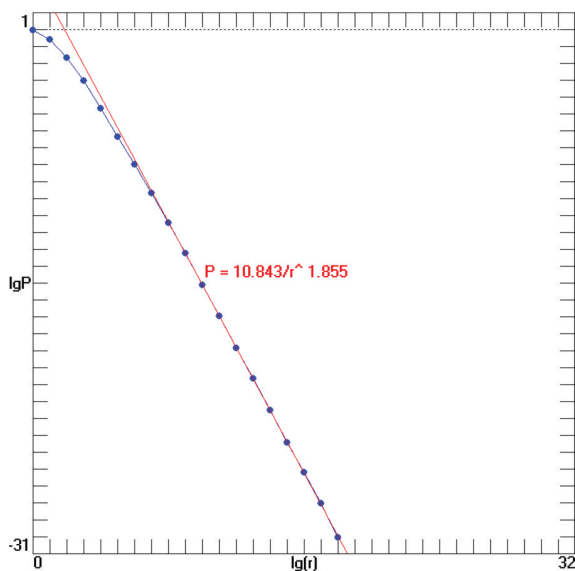
(b)

FIG. 3. The Hénon map has a Class 3 fractal basin that extends to infinity but with a noninteger power law scaling.

(a)

(b)

FIG. 4. The Tinkerbell map has a Class 4 finite basin with a fractal boundary and a size comparable to the size of the attractor.

$$
\begin{aligned}
X_{n+1} &= X_n{}^2 - Y_n{}^2 + aX_n + bY_n \\
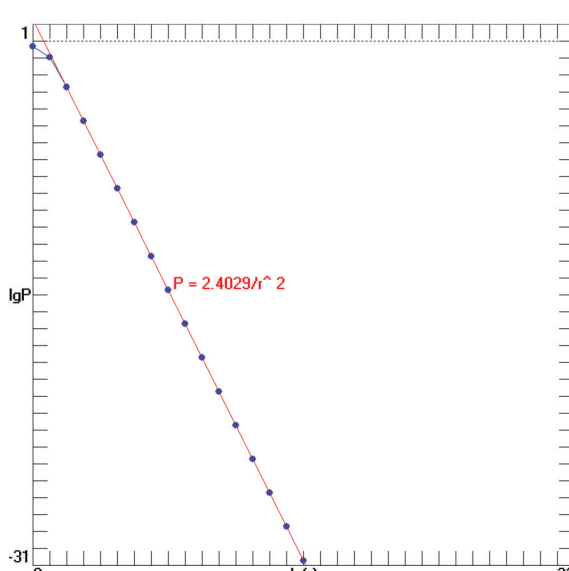Y_{n+1} &= 2X_nY_n + cX_n + dY_n
\end{aligned}
\tag{8}
$$

with parameters $a = 0.9, b = -0.6, c = 2,$ and $d = 0.5,$ as shown in Fig. 4 with Lyapunov exponents $(0.1900, -0.5209)$ and a Kaplan–Yorke dimension of 1.3647. The basin is evidently finite and appears to have a fractal boundary.

The effective radius of the basin is the value of r for which $P(r) = 1$ or $r_0 = \sqrt{P_0} \simeq 1.55$, which is consistent with the fact that the basin is only slightly larger than the attractor in Fig. 4. Such tight fitting basins are common in chaotic systems with Class 4 basins and thus require a careful choice of initial conditions.

Another family of two-dimensional maps with Class 4 fractal basins (but without a strange attractor) are the quadratic Julia sets of the mapping $Z_{n+1} = Z_n{}^2 + C$, where Z and C are complex numbers.[15] Much effort has been devoted to their study as well as to the related Mandelbrot set.[16]

IV. 3-D ORDINARY DIFFERENTIAL EQUATION EXAMPLES

To show that the method is not limited to two-dimensional maps, we show here examples of each of the four classes in chaotic flows governed by autonomous systems of ordinary differential equations (ODEs). Because the basins reside in a three-dimensional state space, we will not attempt to show the shape of the basins, which are normally viewed only in various cross sections.

A. Class 1 basin

Probably, the most familiar example of a three-dimensional chaotic flow is the Lorenz system[19]

$$\dot{x} = 10(y - x)$$
$$\dot{y} = -xz + 28x - y \qquad (9)$$
$$\dot{z} = xy - 8z/3$$

with Lyapunov exponents $(0.9056, 0, -14.5723)$ and a Kaplan–Yorke dimension of 2.0621, which is well known to have a global attractor with a Class 1a basin. Its basin of attraction is the whole of the 3-D state space except for the unstable equilibrium points at $(0, 0, 0)$ and $(\pm\sqrt{72}, \pm\sqrt{72}, 27)$ and the infinitely many unstable periodic orbits embedded in the attractor, which are a set of measure zero. Another system with a Class 1a basin is the Chen system.[20]

As an example of a Class 1b system, we only need to change the 28 to 24 in Eq. (9)

$$\dot{x} = 10(y - x)$$
$$\dot{y} = -xz + 24x - y \qquad (10)$$
$$\dot{z} = xy - 8z/3,$$

which causes the equilibrium points at $(\pm\sqrt{184/3}, \pm\sqrt{184/3}, 23)$ to become stable,[21] and their basins carve out holes in the otherwise global basin of the strange attractor with Lyapunov exponents $(0.7991, 0, -14.4658)$ and a Kaplan–Yorke dimension of 2.0552. The equilibrium points have Class 3 basins of attraction that stretch to infinity but with a probability that decreases approximately as $1/r^{1.8}$ so as to become negligible compared with the basin of the strange attractor at large r. The basin of the strange attractor has a nonmonotonic $P(r)$ with a minimum of about 0.9 at $r \approx 4$, but it is asymptotic to $P(r) = 1$ for large r as required for a Class 1 basin.

B. Class 2 basin

Almost as familiar is the Rössler system[22]

$$\dot{x} = -y - z$$
$$\dot{y} = x + 0.2y \qquad (11)$$
$$\dot{z} = 0.2 + z(x - 5.7)$$

with Lyapunov exponents $(0.0714, 0, -5.3943)$ and a Kaplan–Yorke dimension of 2.0621, which has a Class 2 basin that fills about 23% of the 3-D state space.

C. Class 3 basin

The simplest autonomous system of ODEs with a quadratic nonlinearity and a chaotic solution is given by[23]

$$\dot{x} = y$$
$$\dot{y} = z \qquad (12)$$
$$\dot{z} = -2.017z + y^2 - x$$

with Lyapunov exponents $(0.0551, 0, -2.0721)$ and a Kaplan–Yorke dimension of 2.0266, and its attractor has a relatively small Class 3 basin.

D. Class 4 basin

Class 4 basins appear to be relatively uncommon in simple three-dimensional autonomous chaotic flows. However,

it is possible to convert most chaotic flows into ones with a Class 4 basin by multiplying their right-hand sides by a function $f(x, y, z) = 1 - (x^2 + y^2 + z^2)/R^2$, which is zero on a sphere of radius R and approaches unity toward the center of the sphere. Since the flow is zero on that sphere, trajectories cannot cross it, and hence, the basin must be completely confined within it. If R is sufficiently large, the chaos is preserved by this modification, although the strange attractor may move and change size slightly.

As an example, the method can be applied to the Lorenz system in Eq. (9) with $R = 64$

$$\dot{x} = 10(y - x)f(x, y, x)$$
$$\dot{y} = (-xz + 28x - y)f(x, y, z)$$
$$\dot{z} = (xy - 8z/3)f(x, y, z) \qquad (13)$$
$$f(x, y, z) = 1 - (x^2 + y^2 + z^2)/4096,$$

which remains chaotic. The modified system has a basin whose volume is no larger than $(4\pi R^3/3)$, and thus, it provides a useful check on the accuracy of the Monte Carlo calculation of the basin size.

The Lyapunov exponents change from $(0.9056, 0, -14.5723)$ for $R = \infty$ to $(0.7145, 0, -11.4953)$ for $R = 64$. The ordinary Lorenz system of Eq. (9) is centered on $(0, 0, 23.5495)$ and has a standard deviation of 14.7770, but when the spherical boundary at $R = 64$ is added, the center shifts to $(0, 0, 24.9570)$, and the standard deviation increases to 15.54861. Thus, the attractor appears to expand and move toward the boundary slightly, although it is comfortably inside the boundary. If the basin boundary lies on the sphere, we expect P_0 to have a value of $P_0 = (64/15.54861)^3 = 69.737$, which is in reasonable agreement with the calculated value of 70.098.

V. OTHER EXAMPLES

We conclude with a few other examples of chaotic systems with various basin classes.
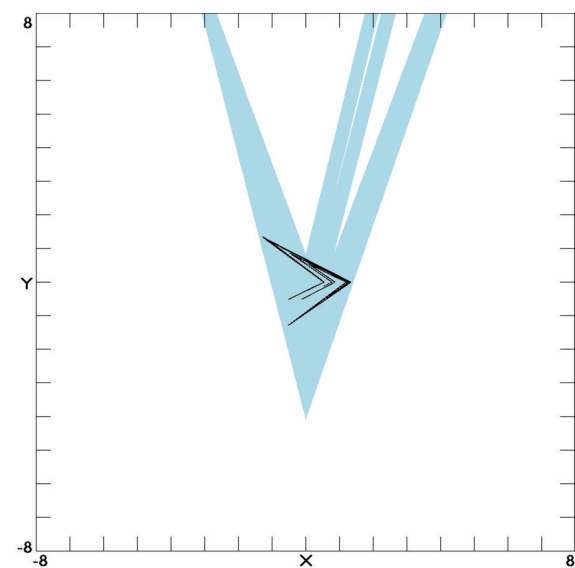
A. Lozi map

The Lozi map[17]

$$X_{n+1} = 1 - 1.7|X_n| + 0.5Y_n$$
$$Y_{n+1} = X_n \qquad (14)$$

shown in Fig. 5 with Lyapunov exponents $(0.4702, -1.1634)$ and a Kaplan–Yorke dimension of 1.4042 resembles the Hénon map with a Class 3 basin with $\gamma = 1.476$, which implies that the dimension of the basin is $D - \gamma = 2 - 1.497 = 0.503$.
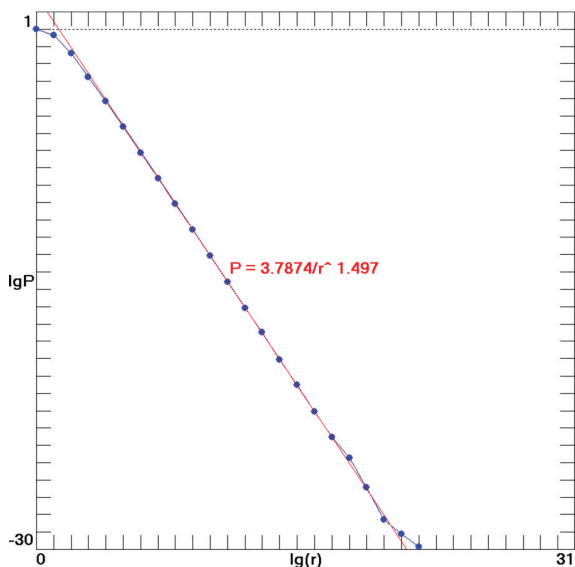
B. Dual Hénon map

An example of a system that has a symmetric pair of strange attractors is the cubic map

$$X_{n+1} = 2X_n + 0.3Y_n - 0.1X_n^3$$
$$Y_{n+1} = X_n \qquad (15)$$

(a)

(b)

FIG. 5. The Lozi map resembles the Hénon map but with angular corners and a Class 3 fractal basin that extends to infinity but with a noninteger power law scaling.
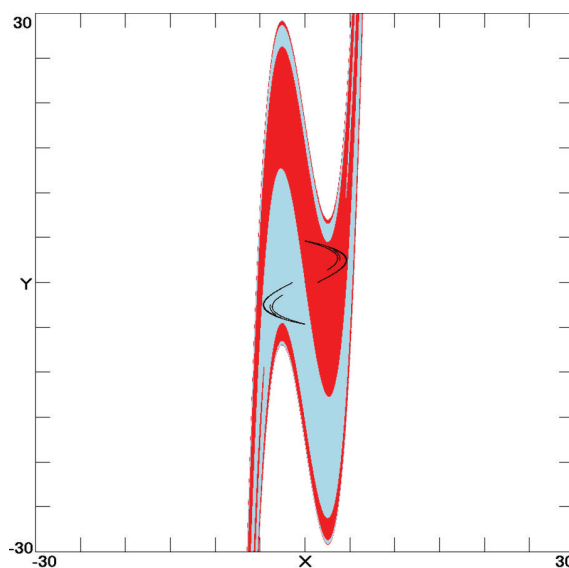

(a)

(b)

FIG. 6. The dual Hénon map has two symmetric Hénon-like attractors, each with a Class 3 fractal basin that extends to infinity but with a noninteger power law scaling.

shown in Fig. 6 with Lyapunov exponents $(0.3524, -1.5563)$ and a Kaplan–Yorke dimension of 1.2264. Each attractor resembles the Hénon map, and each has a Class 3 basin with $\gamma = 1.896$, which implies that the dimension of the basin is $D - \gamma = 2 - 1.896 = 0.104$.
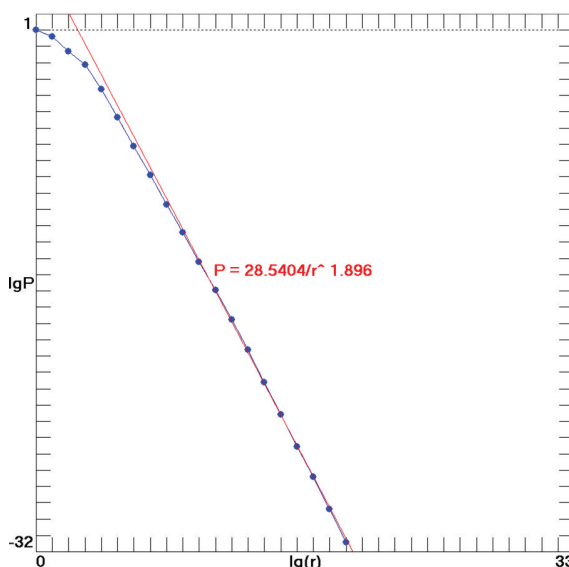
C. Sprott 3-D map

A simple example of a three-dimensional chaotic map from the preface of Ref. 18 is

$$
\begin{aligned}
X_{n+1} &= X_n^2 - 0.2X_n - 0.9Y_n + 0.6Z_n \\
Y_{n+1} &= X_n \\
Z_{n+1} &= Y_n
\end{aligned}
$$
(16)

with Lyapunov exponents of $(0.1275, -0.1504, -0.4879)$ and a Kaplan–Yorke dimension of 1.8476. This is a kind of

three-dimensional generalization of the Hénon map and also has a Class 3 basin with $\gamma = 2.796$, which implies that the dimension of the basin is $D - \gamma = 3 - 2.796 = 0.204$.

D. Rössler hyperchaos

Probably, the best known four-dimensional flow is the one proposed by Rössler[24] to illustrate hyperchaos

$$
\begin{aligned}
\dot{x} &= -y - z \\
\dot{y} &= x + 0.25y + w \\
\dot{z} &= 3 + xz \\
\dot{w} &= 0.05w - 0.5z
\end{aligned}
$$
(17)

with Lyapunov exponents $(0.1120, 0.0211, 0, -24.9312)$ and a Kaplan–Yorke dimension of 3.0053, which has a Class 3 basin in the four-dimensional state space.

TABLE I. Selected chaotic systems with their basins of attraction.

System	Reference	Equation	Type	Class	P_0	γ
Logistic	7	1	1-D map	4	2.3110	1
Sine-sine	This study	5	2-D map	1a	1	0
Ikeda	12	6	2-D map	2	0.0799	0
Hénon	13	7	2-D map	3	10.843	1.855
Lozi	17	14	2-D map	3	3.7969	1.497
Dual Hénon	This study	15	2-D map	3	28.540	1.896
Tinkerbell	14	8	2-D map	4	2.4029	2
Sprott preface	18	16	3-D map	3	10.670	2.796
Lorenz 28	19	9	3-D flow	1a	1	0
Lorenz 24	This study	10	3-D flow	1b	1	0
Rössler	22	11	3-D flow	2	0.2286	0
Simplest quadratic	23	12	3-D flow	3	19.744	2.782
Bounded Lorenz	This study	13	3-D flow	4	70.098	3
Rössler hyperchaos	24	17	4-D flow	3	0.4060	0.408

The extension of the method to even higher dimensions is straightforward, although computationally intensive.

VI. CONCLUSION

We have presented here a simple method for classifying basins of attraction and quantifying their size. Table I summarizes the cases previously described, showing the properties of their basins. We recommend that such a calculation be included as part of the routine description of the attractor for any dissipative dynamical system.

[1] G. A. Leonov, N. V. Kuznetsov, and V. I. Vagaitsev, Phys. Lett. A **375**, 2230 (2011).
[2] G. A. Leonov and N. V. Kuznetsov, Int. J. Bifurcat. Chaos **23**, 1330002 (2013).
[3] S. W. McDonald, C. Grebogi, E. Ott, and J. A. Yorke, Physica D **17**, 125 (1985).
[4] C. Mira, D. Fournier-Prunaret, L. Gardini, H. Kawakami, and J. C. Cathala, Int. J. Bifurcat. Chaos **4**, 343 (1994).
[5] E. Ott, J. C. Sommerer, J. C. Alexander, I. Kan, and J. A. Yorke, Phys. Rev. Lett. **71**, 4134 (1993).
[6] N. Metropolis and S. Ulam, J. Am. Stat. Assoc. **44**, 335 (1949).
[7] R. May, Nature **261**, 459 (1976).
[8] P. Grassberger, J. Stat. Phys. **26**, 173 (1981).
[9] M. Molaie, S. Jafari, J. C. Sprott, and S. M. R. H. Golpayegani, Int. J. Bifurcat. Chaos **23**, 1350188 (2013).
[10] J. C. Sprott, Phys. Lett. A **378**, 1361 (2014).
[11] A. Wolf, J. B. Swift, H. L. Swinney, and J. A. Vastano, Phys. Nonlinear Phenom. **16**, 285 (1985).
[12] K. Ikeda, Opt. Commun. **30**, 257 (1979).
[13] M. Henon, Comm. Math. Phys. **50**, 69 (1976).
[14] H. E. Nusse and J. A. Yorke, *Dynamics: Numerical Explorations* (Springer, New York, 1994).
[15] R. L. Devaney, *A First Course in Chaotic Dynamical Systems: Theory and Experiment* (Addison–Wesley–Longman, Reading, MA, 1992).
[16] B. B. Mandelbrot, Ann. N. Y. Acad. Sci. **357**, 249 (1980).
[17] R. Lozi, J. Phys. (Paris) **39**, C5-9 (1978).
[18] J. C. Sprott, *Chaos and Time-Series Analysis* (Oxford Unversity Press, Oxford, 2003).
[19] E. N. Lorenz, J. Atmos. Sci. **20**, 130 (1963).
[20] G. Chen and T. Ueda, Int. J. Bifurcat. Chaos **9**, 1465 (1999).
[21] S. H. Strogatz, *Nonlinear Dynamics and Chaos*, 2nd ed. (Westview Press, Philadelphia, PA, 2015).
[22] O. E. Rössler, Phys. Lett. A **57**, 397 (1976).
[23] J. C. Sprott, Phys. Lett. A **228**, 271 (1997).
[24] O. E. Rössler, Phys. Lett. A **71**, 155 (1979).